Highly birefringent nematic and chiral nematic liquid crystals

K. L. Woon[a]; M. O'neill[a]; P. Vlachos[b]; M. P. Aldred[b]; S. M. Kelly[b]

[a] Department of Physics, University of Hull, Hull HU6 7RX, UK [b] Department of Chemistry, University of Hull, Hull HU6 7RX, UK

PLEASE SCROLL DOWN FOR ARTICLE

Highly birefringent nematic and chiral nematic liquid crystals

K. L. WOON†, M. O'NEILL*†, P. VLACHOS‡, M. P. ALDRED‡ and S. M. KELLY‡

†Department of Physics, University of Hull, Cottingham Rd., Hull HU6 7RX, UK
‡Department of Chemistry, University of Hull, Cottingham Rd., Hull HU6 7RX, UK

We report a simple interference method to determine the dispersion of the extraordinary refractive index and birefringence of highly conjugated and coloured nematic liquid crystals used as light-emitting materials in organic electroluminescent devices. The measurements are made in the nematic glass phase at room temperature. The birefringence is highly dispersive and values up to 1.1 are obtained. Chiral groups are incorporated into the end chains giving a chiral nematic liquid crystal with a very wide stopband in the visible region. The Berreman matrix method is used to simulate transmission through the chiral nematic liquid crystal cell using the refractive index parameters obtained experimentally. Excellent agreement between theory and experiment is found.

1. Introduction

The Abbé refractometer is widely used to measure the extraordinary and ordinary refractive indices, n_o and n_e, of liquid crystals [1], but is only applicable when these are lower than the refractive index of the prism. Many highly birefringent liquid crystals are required as components of the crystal mixtures used in liquid crystal displays [2–4]. The n_o and n_e of these materials are usually obtained by extrapolating results from mixtures having lower birefringence. Phase contrast spectroscopic methods have been used to measure the refractive index of liquid crystals, [5, 6] but most of these assume that the materials are transparent in the spectral range of interest or that there is a small difference in absorbance for the ordinary and extraordinary rays.

A new class of liquid crystals with birefringence values greater than 0.5 in the visible region has recently been developed to provide light emission for organic light emitting diodes (OLEDs) [7]. These low mass or oligomeric, nematic liquid crystals are coloured with highly polarized absorbance spectra and are designed to have either nematic [8] or nematic glassy phases at room temperature [8–11]. In the latter case glassy films are formed by annealing above the glass transition temperature and quenching to room temperature. Chiral groups can be added to the end chains of nematic liquid crystals to induce a selective reflection band, a so called 1D photonic stopband for circularly polarized light. The spectral width of the stopband of the liquid crystal is proportional to its birefringence, so that this class of liquid crystal is used to induce broad stopbands [12].

Circularly polarized luminescence has been obtained when the stopband overlaps the full luminescence spectrum. Other potential applications include mirrorless 1D photonic stopband lasing [13], circular filters [14] and reflective displays [15]. Many of these light emitting compounds do not mix well with standard low mass nematics so a new method is required to measure their birefringence. Spectroscopic ellipsometry is a high cost method to determine film thickness, the wavelength dependence of n_o and n_e, as well as the anisotropic absorption coefficients [10, 16]. We suggest a modified interference method to obtain n_o and n_e, of highly birefringent and coloured liquid crystals. The validity of the method is proven by comparing the measured and calculated values of the stopband obtained when chiral end groups are substituted in one of the measured liquid crystals.

2. Experimental details

Figure 1 shows the chemical structures of the liquid crystals studied, and table 1 their corresponding transition temperatures. Compounds **a** and **b** are nematic liquid crystals at elevated temperatures and retain nematic glassy phases at room temperature on cooling from the nematic phase. Compound **b** has polymerizable end chains for use in photopatternable OLEDs [17]. Compound **c** is a monotropic chiral nematic liquid crystal with the same aromatic core as **b**. It also retains a room temperature glassy phase on cooling.
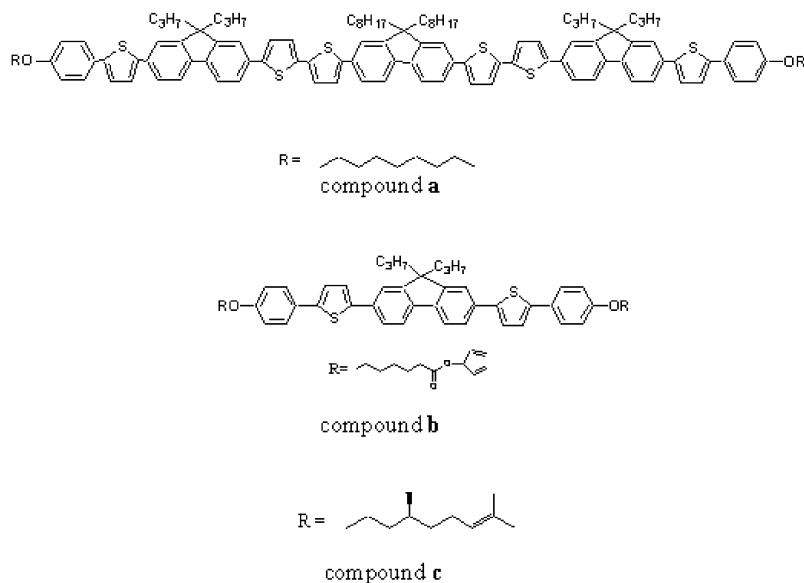
Figure 1. chemical structures of compounds **a** – **c**.

Two kinds of cell are used to measure refractive indices. Both cells consist of glass substrates coated with a rubbed polyimide alignment layer to provide uniaxial homogeneous alignment. Cell **A** is a wedge cell where the direction of alignment is parallel to the direction of increasing thickness. A spacer of 7 μm is used to define the thicker region while only pure UV-curable glue is used at the thin region. The wedge angle of the unfilled cell **A** is found using light from a sodium source of wavelength $\lambda_o = 589$ nm incident normally on the wedge cell. The reflected fringes are observed using a travelling microscope. The wedge angle θ is found from

$$\tan \theta = \frac{N\lambda_o}{2nX} \qquad (1)$$

where N is the number of fringes observed on translating a distance X and n is the refractive index of the medium sandwiched between the wedge cell. For the air-filled wedge, $n = 1.00$. The cells are filled by vacuum-induced capillary flow of compound **a** or **b** in the isotropic phase. Cell **B** is prepared using 2 μm silica spacers to provide a uniform cell gap. The cell gap of the unfilled cell **B** is measured using a broadband light source from a tungsten lamp.

The n_e is first measured at 589 nm with incident light polarized along the extraordinary axis of the liquid crystals. Fringes from the filled wedge cell **A** are measured using the travelling microscope and n_e is found by using equation (1). Figure 2 shows the experimental set-up used to measure n_e. White light polarized along the extraordinary axis is incident via a bifurcated optical fibre onto cell **B** filled with either compound **a** or **b**. It is important to align the extraordinary axis with the polarization direction of the light. This can be done by detecting the transmission of light through the cell placed between crossed polarizers. The cell is rotated until transmission is minimized. The interference pattern from the normal reflections is detected via the second arm of the bifurcated fibre using an Ocean Optic spectrometer. Peaks are observed in the reflected light spectrum when

$$m\lambda = 2n_e d \qquad (2)$$

where m is an integer which can be found by inspection since n_e is known at 589 nm.

The difference between n_o and the refractive index of the polyimide layer is too small to observe reflected fringes when the incident polarization direction is

Table 1. Transition temperature of compounds **a**–**c**.

Compound	T_g		Cr		N		I
a	•	45	•	118	•	210	•
b	•	39	•	92	•	108	•
c	•	29	•	123	(•	122)[a]	•

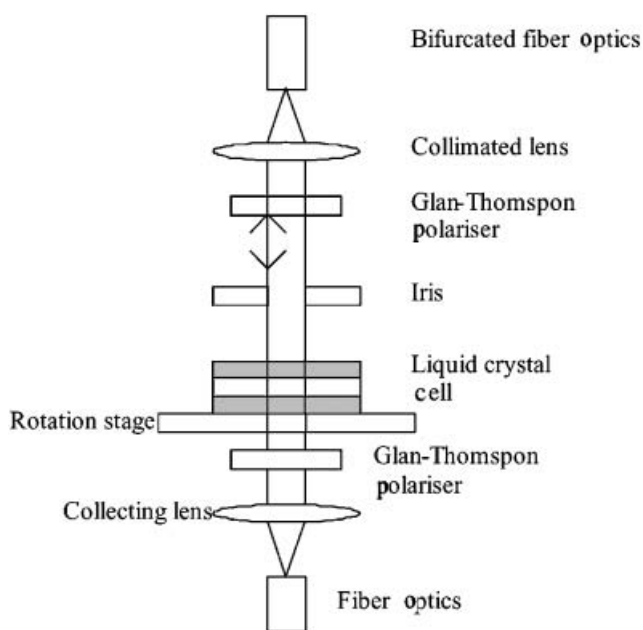[a] Parentheses denote a monotropic mesophase.

Figure 2. experimental set-up for measuring $n_e(\lambda)$ and n_o.

perpendicular to the optic axis. Hence the interference method cannot be used to obtain n_o. However, n_o can be found by considering cell **B** as a retardation plate, if we assume that it is independent of wavelength in the spectral region considered. This assumption would not be valid for most low mass liquid crystals since n_o retains a significant contribution from the transition moment along the axis of the molecule in a macroscopically aligned sample. The magnitude of the contribution depends on the order parameter and is expected to be small for the liquid crystals discussed here, which have high order parameters > 0.8. Spectroscopic ellipsometry shows that a light-emitting oligomeric liquid crystal, which has an order parameter of 0.83, has a dispersion < 0.05 in the equivalent spectral range to our measurements [10]. This confirms that the assumption of a wavelength independent n_o is reasonable. Broadband light polarized at $-45°$ from the optic axis is incident onto filled cell **B** and the intensity is detected after passing through a polarizer at $-45°$ to the optic axis. The transmitted intensity is maximized at wavelengths according to

$$\frac{m\lambda}{d} = n_e - n_o \tag{3}$$

where m is an integer obtained for the different peaks assuming that n_o remains constant over the range of wavelength considered.

Cell **C**, a commercial cell of cell gap $5\,\mu m$ consisting of two glass-ITO substrates coated with a rubbed polyimide alignment layer, is filled with the chiral nematic compound **c**. On cooling, the self-assembly of the uniformly aligned helical structure establishes a 1D photonic stopband, which reflects circularly polarized light with the same sense of circular polarization as the helix over a spectral range matching the helical pitch. The spectroscopic Stokes polarimeter is used to characterize the polarization state of white light from a Xenon lamp on transmission through cell **C**. The Stokes polarimeter consists of a rotating achromatic quarter-wave plate, a fixed Glan–Thomson polarizer and a spectrometer to detect the Stokes parameters for a range of wavelengths. Experimental details are given elsewhere [18]. The Stokes parameter s_3/s is defined as

$$\frac{s_3}{s_o} = \frac{I_R - I_L}{I_R + I_L} \tag{4}$$

where I_L and I_R are the intensities detected when the light passes through a quarter waveplate followed by an analyser set at $+45°$ and $-45°$ from its fast axis, respectively. Hence s_3/s_o is a measure of the circular polarization of the transmitted light. The Berreman Transfer Matrix is used to calculate the theoretical values of s_3/s_o as discussed in detail elsewhere. The refractive index parameters n_e and n_o, obtained from the above measurement of compound **b** are used in the calculations and the numerical results are fitted to the experimental s_3/s_o [18]. The theory takes multiple reflections at the various interfaces of the cells into account. The refractive index of the polyimide is used as a variable parameter.

3. Results and discussion

The n_e values of compounds **a** and **b** are 2.23 and 2.01, respectively at 589 nm using the wedge cell **A**. Equation (2) is then applied to find n_e using cell **B**; n_o is found to be 1.56 and 1.63 for **a** and **b**, respectively. The n_e and Δn of both compounds are plotted as a function of wavelength in figure 3. The highly dispersive nature of n_e results from the $\pi-\pi^*$ absorption resonances which peak at 452 and 395 nm for compounds **a** and **b**, respectively. Cell **B** is thick, so that the short wavelength limit of the measurements is determined by material absorbance. A maximum Δn value of 1.1 is obtained for the fourteen ring compound **a**. For the six-ring compound **b** the corresponding value is 0.7. Hence, as expected, both n_e and Δn_e increase with the conjugation length.

Figure 4 shows the wavelength dependence of the measured and calculated values of the Stokes parameter on transmission of white light through the chiral nematic cell **C**. A broad stopband is observed between 470 and 580 nm. The stopband overlaps the photoluminescence spectrum so that the PL from the cell is
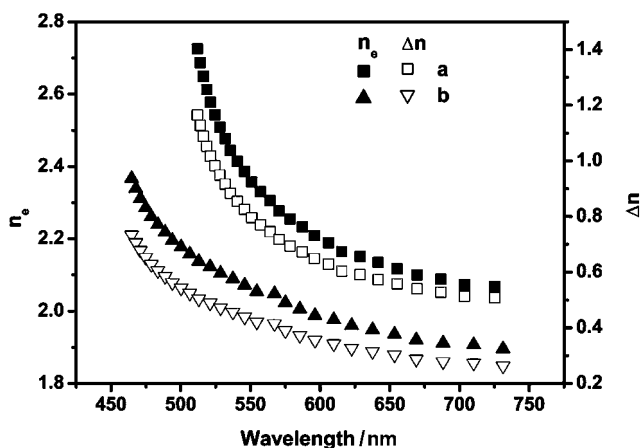
Figure 3. n_e and Δn of compounds **a** and **b** as a function of wavelength.
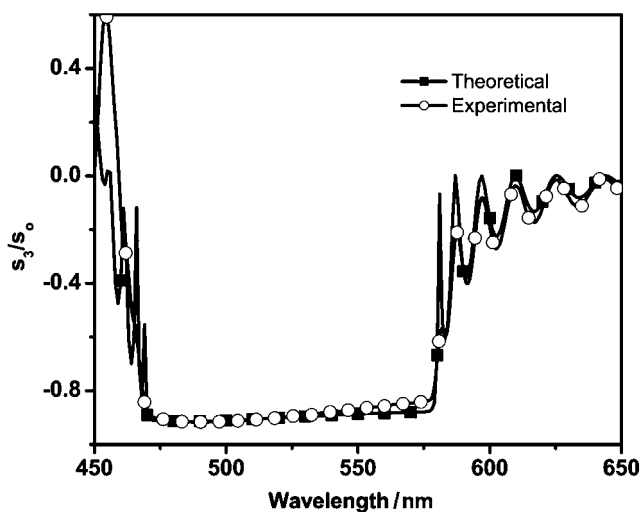
Figure 4.   The experimental and theoretical values of s_3/s_o obtained on transmission of unpolarized light through cell **C** filled with compound **c**.

4.   Conclusions

A simple interference method is suggested to measure n_e and Δn of light-emitting liquid crystal glasses which are highly birefringent and dispersive. Birefringence values up to 1.1 are obtained for these highly conjugated liquid crystals. Both n_e and Δn increase with conjugation length. We show that chiral nematic liquid crystals with spectrally broad stopbands can be produced by incorporating chiral moieties into the end groups of these highly birefringent nematic materials. The values of n_e and Δn obtained for the nematic compound are successfully used to predict the stopband range of the chiral nematic compound using the Berreman matrix method.

highly circularly polarized [12]. Below 460 nm, material absorption affects the measured result of s_3/s_o. At longer wavelengths there is excellent agreement between theory and experiment confirming not only the validity of the assumption that n_o is non-dispersive but also the accuracy of such a simple interference method in measuring n_e. A helical pitch of 288 nm is obtained from the model. It has previously been shown that there is a significant error when the dispersion of n_e is not included in the calculation of the stopband of a transparent chiral nematic liquid crystals in the visible spectral region [19]. Here, no fit to the data could be made when dispersion was neglected because of the proximity of the absorption band to the stopband.

References

[1] W.U. Müller, H. Stegemeyer. *Ber. Bun. Ges.*, **77**, 20 (1972).
[2] S.T. Wu, C.S. Hsu, Y.Y. Chuang, H.B. Cheng. *Jpn. J. Appl. Phys. 2 Lett.*, **39**, L38 (2000).
[3] C. Sekine, K. Iwakura, N. Konya, M. Minai, K. Fujisawa. *Liq. Cryst.*, **28**, 1375 (2001).
[4] C. Sekine, M. Ishitobi, K. Iwakura, M. Minai, K. Fujisawa. *Liq. Cryst.*, **29**, 355 (2002).
[5] S.T. Wu, U. Efron, L.D. Hess. *Appl. Optics*, **23**, 3911 (1984).
[6] M. Warenghem, G. Joly. *Mol. Cryst. liq. Cryst.*, **207**, 205 (1991).
[7] M. O'Neill, S.M. Kelly. *Adv. Mater.*, **15**, 1135 (2003).
[8] M.P. Aldred, A.J. Eastwood, S.M. Kelly, V. Panos, A.E.A. Contoret, S.R. Farrar, B. Mansoor, M. O'Neill, W.C. Tsoi. *Chem. Mater.*, **16**, 4928 (2004).
[9] A.E.A. Contoret, S.R. Farrar, M. O'Neill, J.E. Nicholls, G.J. Richards, S.M. Kelly, A.W. Hall. *Chem. Mater.*, **14**, 1477 (2002).
[10] Y.H. Geng, S.W. Culligan, A. Trajkovska, J.U. Wallace, S.H. Chen. *Chem. Mater.*, **15**, 542 (2003).
[11] M. Jandke, D. Hanft, P. Strohriegl, K. Whitehead, M. Grell, D.D.C. Bradley. *Proc. SPIE*, **4105**, 338 (2001).
[12] K.L. Woon, M. O'Neill, G.J. Richards, M.P. Aldred, S.M. Kelly, A.M. Fox. *Adv. Mater.*, **15**, 1555 (2003).
[13] V.I. Kopp, B. Fan, H.K.M. Vithana, A.Z. Genack. *Opt. Lett.*, **23**, 1707 (1998).
[14] H.P. Chen, D. Katsis, J.C. Mastrangelo, S.H. Chen, S.D. Jacobs, P.J. Hood. *Adv. Mater.*, **12**, 1283 (2000).
[15] W.D. St John, Z.J. Lu, J.W. Doane. *J. Appl. Phys.*, **78**, 5253 (1995).
[16] M. Schubert, B. Rheinlander, C. Cramer, H. Schmiedel, J.A. Woollam, C.M. Herzinger, B. Johs. *J. opt. Soc. Am. A.*, **13**, 1930 (1996).
[17] A.E.A. Contoret, S.R. Farrar, P.O. Jackson, L. May, M. O'Neill, J.E. Nicholls, G.J. Richards, S.M. Kelly. *Adv. Mater.*, **12**, 971 (2000).
[18] K.L. Woon, M. O'Neill, G.J. Richards, M.P. Aldred, S.M. Kelly. *J. opt. Soc. Am. A.*, **22**, 760 (2005).
[19] N.W. Roberts, J.P.S. Guillou, H.F. Gleeson, I. Kirar, S.J. Watson, E.O. Arikainen. *Mol. Cryst. liq. Cryst.*, **411**, 1099 (2004).